

SHAPE COEXISTENCE, TRIAXIAL SHAPE AND BAND TERMINATIONS AT HIGH SPIN*

I. RAGNARSSON^a, B.G. CARLSSON^a, A. KARDAN^{b,c}, HAI-LIANG MA^{a,c}

^aDiv. of Math. Physics, LTH, Lund Univ., P.O. Box 118, 22100 Lund, Sweden

^bSchool of Physics, Damghan University, P.O. Box 36716-41167, Damghan, Iran

^cChina Institute of Atomic Energy, P.O. Box 275-10, Beijing 102413, China

(Received January 16, 2015)

Selected high-spin bands in $A = 120$ – 170 nuclei are interpreted within the configuration-constrained Cranked Nilsson–Strutinsky formalism with pairing neglected (CNS) and with pairing included (CNSB). A few bands in Lu/Hf nuclei which have been interpreted as formed at large triaxial deformation are reinterpreted as rotational bands at small deformation approaching termination. The differences between the linked high-spin rotational bands in $^{125,126}\text{Xe}$ are explored, suggesting that the bands in ^{126}Xe terminate high above yrast at close to spherical shape.

DOI:10.5506/APhysPolB.46.477

PACS numbers: 21.10.–k, 21.10.Pc, 21.60.Cs, 21.60.Ev

1. Introduction

At high spin where pairing is negligible, nuclear rotational bands will generally have a moment of inertia which is close to the rigid body value [1]. Therefore, a large moment of inertia indicates a large deformation, which means that it becomes energetically cheaper to increase the spin value. The rule about the increased deformation should, however, not be applied too literally, because the ‘next spin state’ might also come at a lower energy because of substantial shape changes within the band [2]. Such shape changes occur for configurations having a low collectivity which, in general, means that the corresponding rotational bands are close to termination. We will exemplify this by rotational bands in ^{161}Lu [3] and ^{164}Hf [4].

The linked high-spin rotational bands in $^{125,126}\text{Xe}$ [5, 6] have been interpreted as formed in similar configurations. However, a closer investigation reveals interesting differences [7]. Thus, the bands in ^{125}Xe appear to be

* Presented at the Zakopane Conference on Nuclear Physics “Extremes of the Nuclear Landscape”, Zakopane, Poland, August 31–September 7, 2014.

built in configurations with several neutrons excited across the $N = 82$ gap, while the neutrons remain in the $N = 50$ – 82 valence space for the bands in ^{126}Xe . Therefore, the spin values in the linked bands ^{126}Xe are much more limited. Indeed, these bands reach their maximum spin values and terminate in approximately spherical configurations. It is of special interest that these terminations occur high above yrast where one would not really expect to see any discrete bands.

2. The CNS and CNSB methods

The rotational bands are interpreted in the CNS [2, 8, 9] and CNSB [10, 11] models. Both these models are based on the modified oscillator potential which is cranked around a principal axis. The Strutinsky method is used to calculate the total energy, which is minimized in the $(\varepsilon, \gamma, \varepsilon_4)$ deformation space. Pairing is neglected in the CNS approach which makes it possible to specify configurations in a detailed way, based on the occupation of orbitals which have their main amplitudes in specific j -shells or groups of j -shells. The CNSB approach is based on the Ultimate Cranker formalism [12]. The total energy for the correct number of particles with pairing included (‘particle number projection’) is minimized not only in deformation space but also in a mesh in the pairing parameters, Fermi energy λ and pairing gap Δ . Diabatic configurations are followed. This becomes relatively straightforward because it is done at constant values of the deformation and pairing parameters. The same rotating liquid drop parameters [9] are used in the CNS and CNSB calculations.

3. The X2 band in ^{161}Lu

The level scheme of ^{161}Lu ($Z = 71$, $N = 90$) has been analyzed in the CNS as well as CNSB formalisms [11]. With pairing included in CNSB, the only good quantum numbers are parity π and signature α for protons and neutrons, *i.e.* 16 different configurations can be calculated characterized by $(\pi, \alpha)_p(\pi, \alpha)_n$. We have introduced the same constraint in the CNS calculations and compare the positive parity yrast lines in Fig. 1 [11]. The difference shows a rather smooth trend down to low spin values which suggests that, with a small renormalization of the moment of inertia, experiment should be well described also in the CNS formalism. It appears that paired crossings are important only below $I = 25$ – 30 . Note also that at very high spin, more aligned (terminating) states are calculated with pairing included.

So-called triaxial superdeformed (TSD) bands have been observed in the Lu isotopes with $N = 90$ – 96 , [13–15]. In some cases, the triaxial shape has been verified by the identification of wobbling bands [13]. Two TSD bands

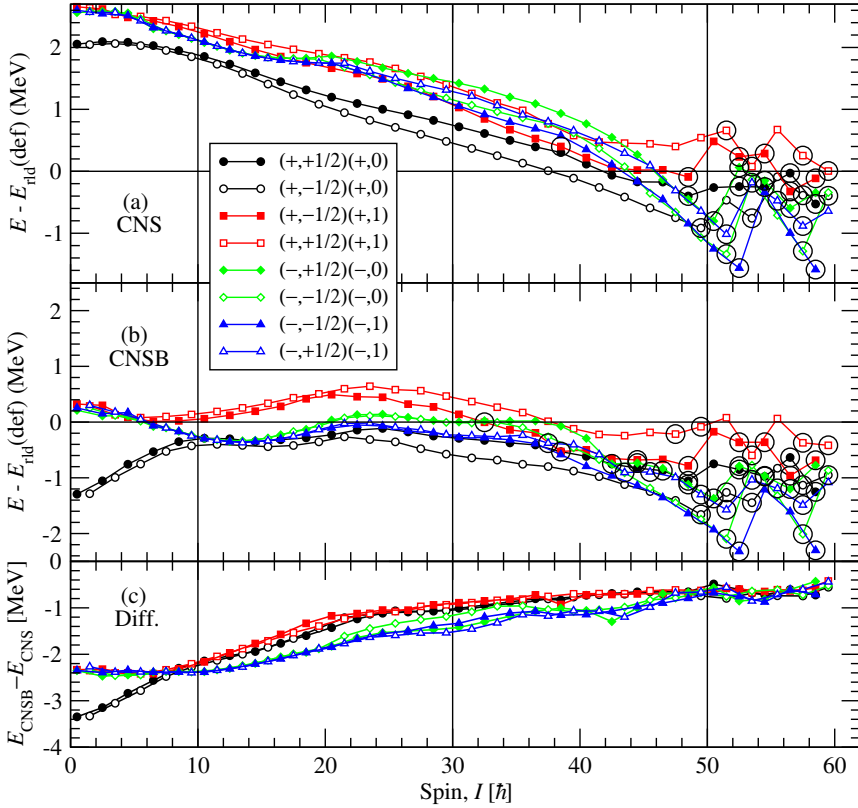


Fig. 1. The energies of ^{161}Lu calculated in the CNS and CNSB models for positive parity configurations are shown relative to the rotating liquid drop energy in panels (a) and (b), respectively, with the difference between the two calculations in panel (c). Aligned states are encircled.

have been observed in ^{161}Lu [3, 16]. In addition, another band, X2, with a moment of inertia that is very similar to that of the TSD bands is also present in the level scheme. In Ref. [3], it is suggested that this band is also formed at triaxial shape but at a somewhat reduced and ‘less collective’ deformation. The corresponding minimum is, however, calculated rather high in energy. It is, therefore, satisfying that in a subsequent analysis [17], it was concluded that the energy of this band is well described by a configuration approaching termination at $I = 49.5^+$. One should note that ^{161}Lu has 90 neutrons which is a favoured particle number for terminating bands [18] even though such bands have previously been identified only for smaller proton numbers [2]. The terminating band interpretation is also more likely in the sense that it is then much easier to understand why the band is linked with the normal deformed bands, namely the [404] 7/2 band. Indeed, it was

recently concluded [11] that in the transition from the [404] 7/2 band to the X2 band, one proton is deexcited from the [431] 3/2 orbital to the [404] 7/2 orbital, *i.e.* from an orbital of $d_{3/2}$ character to an orbital of $g_{7/2}$ character. This detailed understanding is obtained in the unpaired CNS formalism but it is confirmed with pairing included in the CNSB formalism. The active configurations are schematically illustrated in Fig. 2 where one notes that the ^{146}Gd core is closed in the configuration of the X2 band, *i.e.* this band is built from the 15 valence particles outside the core. Using the labels in Fig. 1, it is of the type $(\pi, \alpha)_p(\pi, \alpha)_n = (+, -1/2)(+, 0)$. In both CNS (upper panel) and CNSB (middle panel), this band is calculated lowest in energy among the positive parity configurations in an extended spin range, $I \approx 20\text{--}45$.

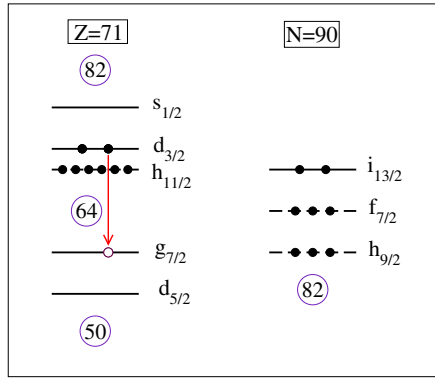


Fig. 2. The configuration of the [404] 7/2 band of ^{161}Lu at high spin where pairing is less important. The approximate occupation of the different j -shells ($\pi h_{11/2}$, $\nu i_{13/2}$ or groups of j -shells ($\pi d_{5/2}g_{7/2}$, $\pi d_{3/2}s_{1/2}$, $\nu h_{9/2}f_{7/2}$) is illustrated relative to a $Z = 64$, $N = 82$ core where particles are shown by filled circles and holes by open circle. The configuration change when the X2 band is created is shown by an arrow, *i.e.* a particle in the [431] 1/2 orbital of $d_{3/2}s_{1/2}$ character is moved to the [404] 7/2 orbital of $d_{5/2}g_{7/2}$ character closing the core.

4. The bands labelled TSD1 and TSD2 in ^{164}Hf

Two high-spin signature-degenerate rotational bands were recently observed [4] in ^{164}Hf ($Z = 72$, $N = 92$). Mainly based on their large moment of inertia, they were interpreted as triaxial superdeformed (TSD) bands and labelled TSD1 and TSD2. Such bands have been predicted since long in the Hf isotopes. However, there are several features which do not support the TSD interpretation of the observed bands. First, both bands are linked by two transitions to the normal-deformed AE and AF bands, *i.e.* bands with one odd neutron in the $i_{13/2}$ shell and another in the $h_{9/2}f_{7/2}$ shells.

Therefore, one would expect that the new ‘TSD’ bands have a similar configuration as the AE and AF bands, *i.e.* it is unlikely that these new bands are formed in a considerably more deformed TSD minimum. Furthermore, in Ref. [4], the lowest calculated bands in the TSD minimum with correct parity and signature are around 1 MeV higher in energy than the observed ‘TSD’ bands and they are not signature degenerate.

In the unpaired formalism, the relevant configurations which correspond to the AE and AF bands will have 3 $i_{13/2}$ neutrons and either 6 or 8 $h_{11/2}$ protons (*cf.* Fig. 2). All other configurations with an odd number of $i_{13/2}$ neutrons and an even number of $h_{11/2}$ protons will come much higher in energy. In the calculations, it is not so evident which single-particle parameters to use. So-called $A = 150$ parameters [19] have generally been used for the terminating bands around $^{158}\text{Er}_{90}$, while standard parameters [8] appear more appropriate for the nuclei in the middle of the deformed rare earth region. Because ^{164}Hf comes somewhere in between, both parameter sets are tried in Fig. 3, where the rotational bands are drawn relative to the rotating liquid drop reference. The $\pi(h_{11/2})^8$ band comes lowest or close to lowest at low spin but becomes energetically unfavoured at high spin. Thus, it appears that the major components of the AE and AF bands should be as-

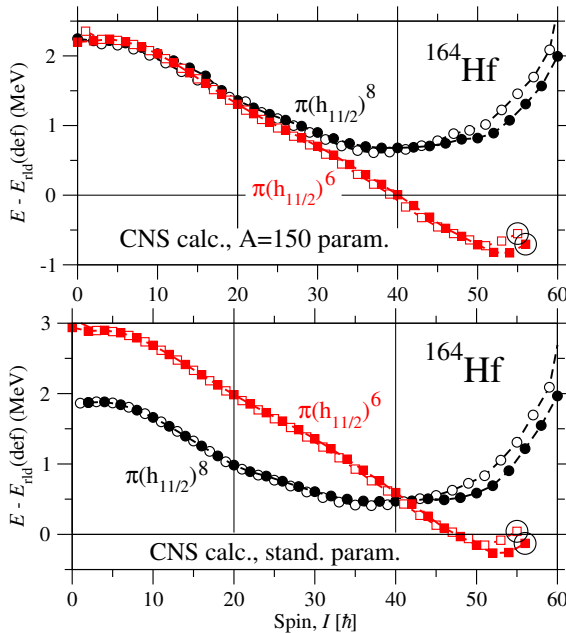


Fig. 3. The calculated energy of the $\pi(h_{11/2})^n\nu(i_{13/2})^3$ ($n = 6, 8$) configurations in ^{164}Hf are shown *versus* spin with a rotating liquid drop reference subtracted. The CNS model has been used with $A = 150$ and standard parameters, respectively.

signed to this configuration. Furthermore, the $\pi(h_{11/2})^6$ bands are strongly down-sloping for almost all spin values corresponding to a large moment of inertia similar to that of the observed ‘TSD1’ and ‘TSD2’ bands. Thus, it seems natural to assign the $\pi(h_{11/2})^6$ bands to the ‘TSD1’ and ‘TSD2’ bands.

In Fig. 3, one notes that the crossing between the $\pi(h_{11/2})^8$ and the $\pi(h_{11/2})^6$ bands is strongly dependent on parameters. One would expect that the parameters for ^{164}Hf should come somewhere between the two parameters sets in Fig. 3. Indeed, it turns out that if the κ and μ parameters are chosen as the arithmetic average of the $A = 150$ and standard parameters, the crossing between the two bands comes at approximately the same spin value as the observed crossing between the AE, AF bands and the ‘TSD1,2’ bands. This is demonstrated in Fig. 4 where the observed bands are shown in the upper panel; those calculated with the intermediate pa-

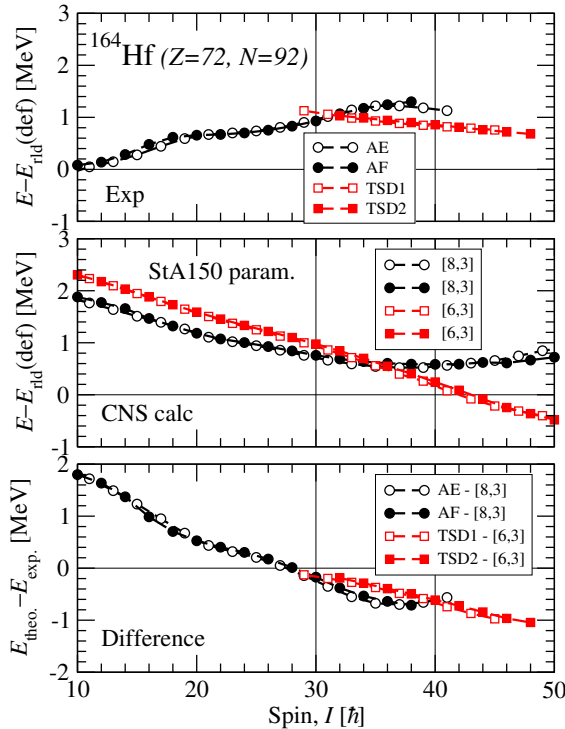


Fig. 4. The observed AE, AF and ‘TSD1,2’ bands in ^{164}Hf (upper panel) compared with the calculated [8,3] and [6,3] bands with the difference between calculations and experiment in the lower panel. The bands are calculated in the CNS model with parameters intermediate between standard and $A = 150$. They are labelled by the number of $h_{11/2}$ protons and $i_{13/2}$ neutrons.

rameters (StA150 param.) in the middle panel and the difference between calculations and experiment in the lower panel. This difference comes out as smoothly decreasing as one would expect when pairing is neglected. Indeed, in CNSB calculations where the present CNS configurations correspond to $(\pi, \alpha)_p(\pi, \alpha)_n = (+, 0)(-, 0)$ and $(+, 0)(-, 1)$, respectively, the difference comes close to constant as a function of spin giving further support to the present interpretation. Furthermore, the energy surfaces at high spin, where pairing is of minor importance are very similar, see Fig. 5.

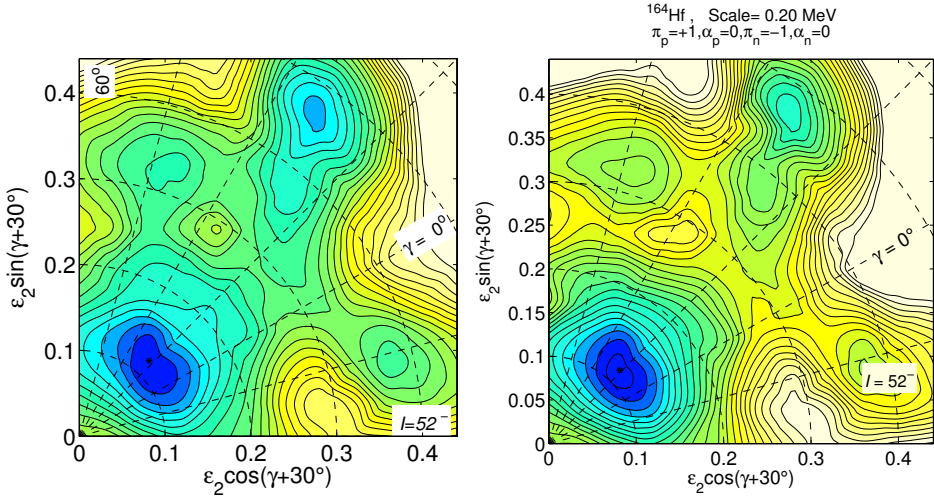


Fig. 5. Calculated total energy surfaces using CNS (left) and CNSB (right), respectively, for the $(\pi, \alpha)_p(\pi, \alpha)_n = (+, 0)(-, 0)$ configuration at $I = 52$ in ^{164}Hf . Note that the relevant configuration at low spin values, $\pi(h_{11/2})^6\nu(i_{13/2})^3$, terminates at $I = 56$.

Our conclusion is thus that the assignment of these high-spin bands as configurations approaching termination is consistent with all observations:

- The large moment of inertia corresponding to a down-slope when drawn relative to the rotating liquid drop energy is reproduced.
- These configurations are calculated low in energy.
- Two signature degenerate bands are calculated.
- The $\pi(h_{11/2})^8$ and $\pi(h_{11/2})^6$ configurations will mix due to pairing correlations making it natural that they are easily linked. Note that it is a common feature that the number of high- j particles change in paired band-crossings, see *e.g.* Refs. [20] and [21].

Our analysis suggests that these bands should rather be labelled TB1 and TB2 (Terminating Bands), but it is, of course, important to measure their life-times. The proposed configuration relative to a ^{146}Gd core can be written as

$$\pi \left[(h_{11/2})_{18}^6 (d_{3/2} s_{1/2})_2^2 \right]_{20} \nu \left[(f_{7/2} h_{9/2})_{18.5, 19.5}^7 (i_{13/2})_{16.5}^3 \right]_{35, 36},$$

where the maximum spin in the different (groups of) j -shells is given as subscript. Thus, the I_{\max} value for the full configuration is $55, 56\hbar$, which should be compared with the highest observed spin, $48\hbar$. In the I_{\max} states, the spin vectors of 18 particles outside the ^{146}Gd core are aligned.

5. The linked high-spin bands in $^{125,126}\text{Xe}$

High-spin bands with known spin values and excitation energies have been observed in $^{125,126}\text{Xe}$ [5, 6]. The bands in these two nuclei show interesting differences as seen clearly in Fig. 6 where they are drawn relative to the standard rotating liquid drop reference [9]. Thus, for $I \approx 55$, the bands in ^{125}Xe are much lower in energy than those in ^{126}Xe . On the other hand, collective yrast bands in neighbouring nuclei should come at similar energies in an analogous manner as nuclear masses in deformed regions show small and regular variations as functions of Z or N when drawn relative to a liquid drop energy. Thus, the yrast bands in ^{126}Xe should be located at similar energies as the observed bands in ^{125}Xe , *i.e.* the observed bands in ^{126}Xe are 3–3.5 MeV above yrast at the highest observed spin value, $I = 56$. The high excitation energy of these states suggests that their configurations are very different from those of the yrast states.

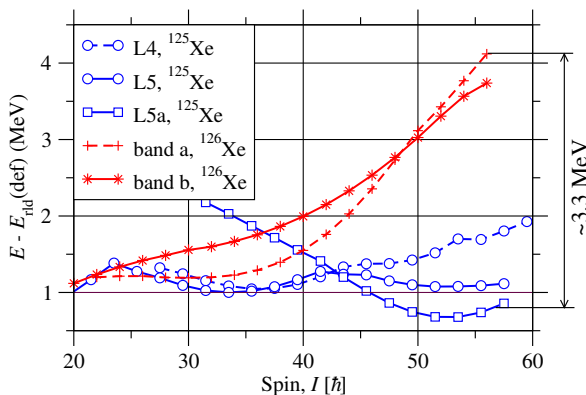


Fig. 6. Observed high-spin bands with known spin and excitation energy in $^{125,126}\text{Xe}$. The energies are shown relative to the standard rotating liquid drop reference [9] calculated for the respective nuclei.

Noting that collective bands in $Z = 50$ – 54 nuclei are generally formed with two $g_{9/2}$ proton holes in the $Z = 50$ core, we have carried out CNS calculations and constructed potential energy surfaces with this constraint as exemplified for $I = 20, 36, 48$ in Fig. 7. There are two minima in these

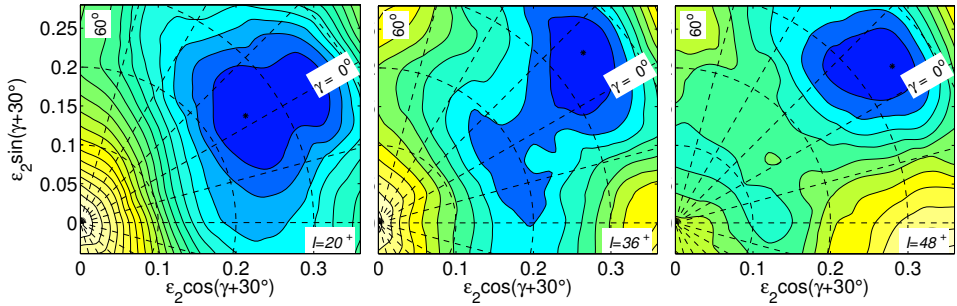


Fig. 7. Calculated total energy surfaces for ^{126}Xe with positive parity. $\pi = +$ and signature $\alpha = 0$ (even spin) with the additional constraint of two proton holes in $g_{9/2}$ orbitals. The contour line separation is 0.5 MeV.

surfaces; one with a deformation $\varepsilon = 0.30$ – 0.35 and another which moves towards smaller deformation coming higher in energy when the spin increases. This minimum becomes very shallow for $I \approx 50$ and disappears at somewhat higher spin values suggesting some kind of termination close to $I = 60$. Our interpretation is then that the bands in ^{125}Xe are built in the more deformed minimum corresponding to configurations with neutrons excited across the $N = 82$ gap (similar to the interpretation in Refs. [5, 6] for the bands in both ^{125}Xe and ^{126}Xe), while the bands in ^{126}Xe are built in the smaller deformation minimum corresponding to neutron configurations in the $N = 50$ – 82 valence space. Life-time measurements [5] support that band L5a in ^{125}Xe should be assigned to the more deformed minimum but are at too low spin values to be decisive in ^{126}Xe . Note that $I = 56$ corresponds to the highest even spin values possible for valence space configurations as exemplified by the configuration (relative to $Z = 50$, $N = 64$) predicted for the $I = 56^+$ state

$$\pi \left[(g_{9/2})_8^{-2} (g_{7/2} d_{5/2})_{10}^4 (h_{11/2})_{10}^2 \right]_{28} \nu \left[(g_{7/2} d_{5/2})_{8.5}^{-3} (h_{11/2})_{18}^6 (d_{3/2} s_{1/2})_{1.5}^5 \right]_{28}.$$

It is of special interest that these I_{max} states are observed, although they are at a high excitation energy.

It is interesting to compare with the unlinked ultra-high spin states in ^{158}Er and neighbouring nuclei [22, 23]. They might be assigned to two different triaxial minima, where the larger deformation minimum is associated with a higher spin value than the lower deformation minimum [24, 25]. This

has similarities to the bands in $^{125,126}\text{Xe}$, *i.e.* the linked bands in ^{126}Xe , which have a smaller spin at a fixed frequency than those in ^{125}Xe , are associated with a smaller deformation than the linked bands in ^{126}Xe .

This work was supported by the Swedish Research Council.

REFERENCES

- [1] A. Bohr, B.R. Mottelson, *Phys. Scr.* **10A**, 13 (1974).
- [2] A.V. Afanasjev, D.B. Fossan, G.J. Lane, I. Ragnarsson, *Phys. Rep.* **322**, 1 (1999).
- [3] P. Bringel *et al.*, *Phys. Rev.* **C73**, 054314 (2006).
- [4] J.C. Marsh *et al.*, *Phys. Rev.* **C88**, 041306 (2013).
- [5] A. Al-Khatib *et al.*, *Phys. Rev.* **C83**, 024306 (2011).
- [6] C. Rønn Hansen *et al.*, *Phys. Rev.* **C76**, 034311 (2007).
- [7] I. Ragnarsson *et al.*, Int. Nucl. Phys. Conf. INPC 2013, <https://agenda.infn.it/internalPage.py?pageId=0&confId=5998>, contrib. NS 185.
- [8] T. Bengtsson, I. Ragnarsson, *Nucl. Phys.* **A436**, 14 (1985).
- [9] B.G. Carlsson, I. Ragnarsson, *Phys. Rev.* **C74**, 011302(R) (2006).
- [10] B.G. Carlsson *et al.*, *Phys. Rev.* **C78**, 034316 (2008).
- [11] Hai-Liang Ma, B.G. Carlsson, I. Ragnarsson, H. Ryde, *Phys. Rev.* **C90**, 014316 (2014).
- [12] T. Bengtsson, *Nucl. Phys.* **A496**, 56 (1989).
- [13] S. Ødegård *et al.*, *Phys. Rev. Lett.* **86**, 5866 (2001).
- [14] G. Schönwasser *et al.*, *Phys. Lett.* **B552**, 9 (2003).
- [15] H. Amro *et al.*, *Phys. Lett.* **B553**, 197 (2003).
- [16] P. Bringel *et al.*, *Eur. Phys. J.* **A16**, 155 (2003).
- [17] I. Ragnarsson, B.G. Carlsson, H. Ryde, *Int. J. Mod. Phys.* **E19**, 590 (2010).
- [18] J. Simpson *et al.*, *Phys. Lett.* **B327**, 187 (1994).
- [19] T. Bengtsson, *Nucl. Phys.* **A512**, 124 (1990).
- [20] F. Grümmer, K.W. Schmid, A. Faessler, *Nucl. Phys.* **A326**, 1 (1979).
- [21] T. Bengtsson, I. Ragnarsson, *Phys. Lett.* **B163**, 31 (1985).
- [22] E.S. Paul *et al.*, *Phys. Rev. Lett.* **98**, 012501 (2007).
- [23] X. Wang *et al.*, *Phys. Lett.* **B702**, 127 (2011).
- [24] A. Kardan, I. Ragnarsson, H. Miri-Hakimabad, L. Rafat-Motevali, *Phys. Rev.* **C86**, 014309 (2012).
- [25] A.V. Afanasjev, Yue Shi, W. Nazarewicz, *Phys. Rev.* **C86**, 031304(R) (2012).